



# Numerical analysis of the aerodynamic performance on wings with morphed trailing edges for MAV applications

Kishore Kumar Sandan<sup>1</sup> · Srinivas Pendyala<sup>1</sup>

Received: 10 December 2022 / Accepted: 22 January 2023 / Published online: 9 February 2023  
© The Author(s), under exclusive licence to Springer-Verlag France SAS, part of Springer Nature 2023

## Abstract

Wing morphing can improve aircraft performance at various periods of flight. Furthermore, exploration was restricted due to restrictions in aerodynamic performance parameters of the morphed wing from such a flexible trailing edge. The continuous morphing of the variable trailing edge has been simulated using the computational fluid dynamic approach and java foil tools. Current research has focused on stable aerodynamic features of morphing wings with morphing trailing edges. The influence of (AoA)-the angle of attack and deflection angle of aerodynamic forces and moments has been studied. A technique for delaying stalling was developed using the morphing trailing edge wing's aerodynamic features. The computational results indicate that the coefficient of lift in the deflecting process is less significant at a low AoA-angle attack than in the static scenario. Increasing the deflection rate then increases the lift coefficient and decreases the drag coefficient. However, the lift coefficients are more significant for greater angles of attack than in the static position and drag, and when it rises as the deflection increases, the rate. Furthermore, the systematic deviation of the morphing trailing edge with a slight deflection angle and a high deflecting rate can increase the lift, drag, and lift-to-drag ratio.

**Keywords** Aerodynamics efficiency · Reynolds number · Coefficient of lift and drag · Coefficient of pressure · Morphing two-dimensional wing · The lift-to-drag ratio

## 1 Introduction

The morphing wing has lately received much interest thanks to the development of innovative materials and sophisticated control structures. Through individual phases of flight, such as various segments, i.e., take-off, cruise, and descent, the aerodynamic shape of a morphed wing can be altered. Several morphed wing designs were developed to improve aircraft efficiency. The aerodynamics, reap its benefits, actuation, and optimization of altering wing configurations were all investigated. Li et al. [1] came up with a list of very well-morphed approaches and model construction and analysis methods for morphed wings. Koreanschi et al. [2] studied an airfoil with a morphing wingtip using a two-dimensional CFD approach, and wind tunnel investigational data and mathematical model results verified their findings. Gabor et al. [3] discovered a reasonable understanding between

CFD findings and a trial wind tunnel test for a morphed airfoil or wing in the pressure distribution. Currently, investigators employ the CFD approach to analyze morphing wings with extensible trailing edges. The CFD technique was used by Abdessemed et al. [4] to investigate the flow characteristics of the aerodynamics of morphing wings relying on the Naca 2412 symmetrical airfoil, and the results revealed that the morphing behavior affects fluid flows. Ai et al. [5] and Jawahar et al. [6] The RANS model was combined well with SA turbulent model to investigate the post properties of routine parameters and stalling of such a Naca 0012 symmetric aerofoils to the adjustable trailing edge and the DES was also used to investigate the aerodynamic efficiency of the morphed wings. Lim and Kim [7] employed an increased bidirectional local search method to improve resolution. Jeong and Kim [8] employed a genetic algorithm to optimize thick airfoils and the Akima curve fitting method to parameterize them. They improved the lift-to-drag ratio by 20–30% associated with the baseline airfoil. Tandis and Assareh [9] employed a honeybee algorithm based on genetics (GBBA). This approach used crossover and community searching operators developed from the genetic and bee

✉ Kishore Kumar Sandan  
kishaero7@gmail.com

<sup>1</sup> Department of Mechanical Engineering, School of Technology, GITAM University, Hyderabad 502329, India

algorithms. It aids in the acceleration of convergence. Yang et al. [10] experimented using Bézier curve characterization and radial basis interpolation. For aerodynamic modification, they employed an optimization technique. Sun et al. investigated the reversed geometry of airfoils. Fincham and Friswell [11] examined a morphing program called Fishbone Active Camber. The method enables the airfoil shape to respond to a broad range of aircraft conditions, leading to optimal results. They used a genetic algorithm for improvement and radial basis interpolation for continuous shape changes. Della Vecchia et al. [12] investigated improving the airfoil form by combining PRS parameterization with a prepared-to-change. The procedure entails determining the compromise solution and the airfoil shape modification's direction. Mukesh et al. [13] improved the NACA 2411 airfoil geometry using the PAR-SEC geometry prediction model, Panel method, and optimization algorithm to enhance the lift force. They validated the improved airfoil in the wind tunnel. Salunke et al. [14] explored the Bezier curve, PAR-Sec techniques, and the combination of Bezier-PAR-Sec techniques for many airfoils. Ebrahimi and Jahangirian [15] developed flexible estimation and an optimization algorithm. Melin [16] used a series of parameterized Bezier curves to define the airfoils.

CFD was used by Niu et al. [17] to analyze the aerodynamic efficiency of airfoils in transonic conditions. However, primarily when, low deflect angles and a consistent initial position for the morphing portion at  $0.7 x/c$  were accounted for. Dumont [18] refined the aerodynamic shape of morphing wings employing CFD at a Mach value of 0.75. At  $Cl = 0.52$ , it was observed that enhancing the angle-of-attack and trailing edge deflect culminated in a  $+ 2.6\%$  lift-to-drag proportion increase. Recently, the theoretical implications of morph techniques in the supersonic domain have also been studied using CFD.

The primary goal of the research is to develop an initial design that could be considered for occurrences based on how the flow field interacts around the aerofoil. The airflow flow can be analyzed utilizing this method, then the lifted devices' aerodynamic characteristics will be obtained. The studies of Zhou et al. [19], Woods et al. [20], and Huntley et al. [21], while additional authors are generally focused on the analysis of the aerodynamic behavior to establish a preliminary concept of the morph aerofoil, but they all accept this assumption. This research aims to offer an airfoil improvement strategy and confirm the results of the CFD analysis. The Bezier slope is created to make the model adjustable in this investigation. The conceptualization method includes control points utilized during the optimization technique. Two of these control points are placed at the airfoil initiation and tip. The other baselines are modified to create the optimized airfoil design during the optimization study. Despite the reality that as much research has been done on morphing wings, more investigation into the aerodynamic efficiency of morphing wings on

a variable trailing edge appears to be needed to apply micro aerial vehicle designs. The steady aerodynamics of the morphed two-dimensional airfoil with a variable trailing edge were simulated using the CFD techniques to bridge that gap.

These modification and optimization activities are carried out using the Java foil and CFD tools. The instruments utilized in this study are used for evaluation. The following is a synopsis of the original research design. Section 1 describes the method for modifying aerodynamic shape using Bezier curves, an optimization method, and the procedure's deployment. The mesh generation method is given. Section 2 analyses and presents the findings of the CFD study. Finally, the study findings are given as micro aerial vehicle application.

## 2 Methodology

### 2.1 Methods for the optimization of the shape and size of the airfoil

Most methods for altering the curvature of an aerofoil or wing can effectively control micro aerial vehicles in various settings during take-off and other combat phases. Despite their differences in execution, most morphing methods were designed to operate or adjust the curvature profile in two-dimensional configurations. Variations in the wing's curvature, such as the leading edge, might differ depending on the procedures. The whole wing is a single control surface for the vehicle's leading edge's morphing aerodynamic profile. Like flaps and slats, other controls are utilized in a typical wing configuration to unfold to have a lift coefficient in an airfoil configuration.

### 2.2 Airfoil shape optimization

There are two structural approaches in the proposed aerodynamic methodology: the standard aerodynamic design method and the inverted design method (Sun et al. [22]). The first design technique involves obtaining aerodynamic performance for a specific airfoil using CFD analyses or experiments and then improving the airfoil shape. These processes are usually performed until the intended results are achieved. The airfoil geometry is determined using the second design method, which would be based on supplied aerodynamic performance. The conventional aerodynamic design approach is applied in this investigation. Multiple values are needed during the optimization method and modifications to the airfoil shape. Darwin's natural evolution hypothesis is the basis for evolutionary computation, a population-based optimization technique. The primary foundations of this philosophy are natural selection and survival.

Natural selection processes are replicated by evolutionary computation, selecting the best solutions of Morphing wings.

### 2.3 Model and numerical methods

A two-dimensional NACA 0018 and NACA 2312 airfoil with a variable trailing edge was posed for simulation analysis. Under the literature, the offset shape is conical, and the flexible zone is 25% of the chord's trailing edge (kaul et al. [23]). In Fig. 1a, shown as a conventional and variable trailing edge is depicted. Despite the reality that as much research has been done on morphing wings, more investigation into the aerodynamics of changing wings of (T.E) with an elastic trailing edge appears to be needed to apply micro aerial vehicle designs. The steady aerodynamics of the morphed wing with a variable trailing edge have been investigated using CFD techniques to bridge that gap. The content of this work is arranged in the following manner. Discusses the numerical methods and validation while discussing the steady and different cases of deflection angles of trailing edge airfoil aerodynamic properties of a morphing wing. The study's findings are reported in Sect. 3.

### 2.4 Geometry

An airfoil model of NACA-2312 with a length of the chord  $c$  of 0.2 m and a span length of 0.4 m was created using Java foil. Toward studying the two-element camber morphing concept, NACA-0012, i.e., a conventional symmetric airfoil, and NACA 2312, an asymmetric airfoil, were chosen as base airfoil and test airfoils. Tests were performed on many trailing-edge profiles and angles of the flap. In two-dimensional airfoils with or without MTE, develop deflection angles said to be the ratio between the morphing flap and the trailing edge modeling. This study used a rigid rectangular cantilevered wing configuration of NACA 0012 to develop a numerical model with chord length  $c = 0.2$  m. The trailing-edge section of the airfoil is interchangeable and has a chord-wise length of 0.06 m. Camber morphing airfoils were designed with a chord of 0.4 m and the same thickness. NACA 0012 has no camber, while NACA 2312 has a camber of 20%. A cubic curve to 15% of the chord makes up the curvature of the mean camber line of NACA 2312. A morphed airfoil was generated nearly identical in shape to NACA 2312 when the NACA 0012 airfoil was morphed. The steady two-dimensional morphing trailing edge Profile NACA 2312

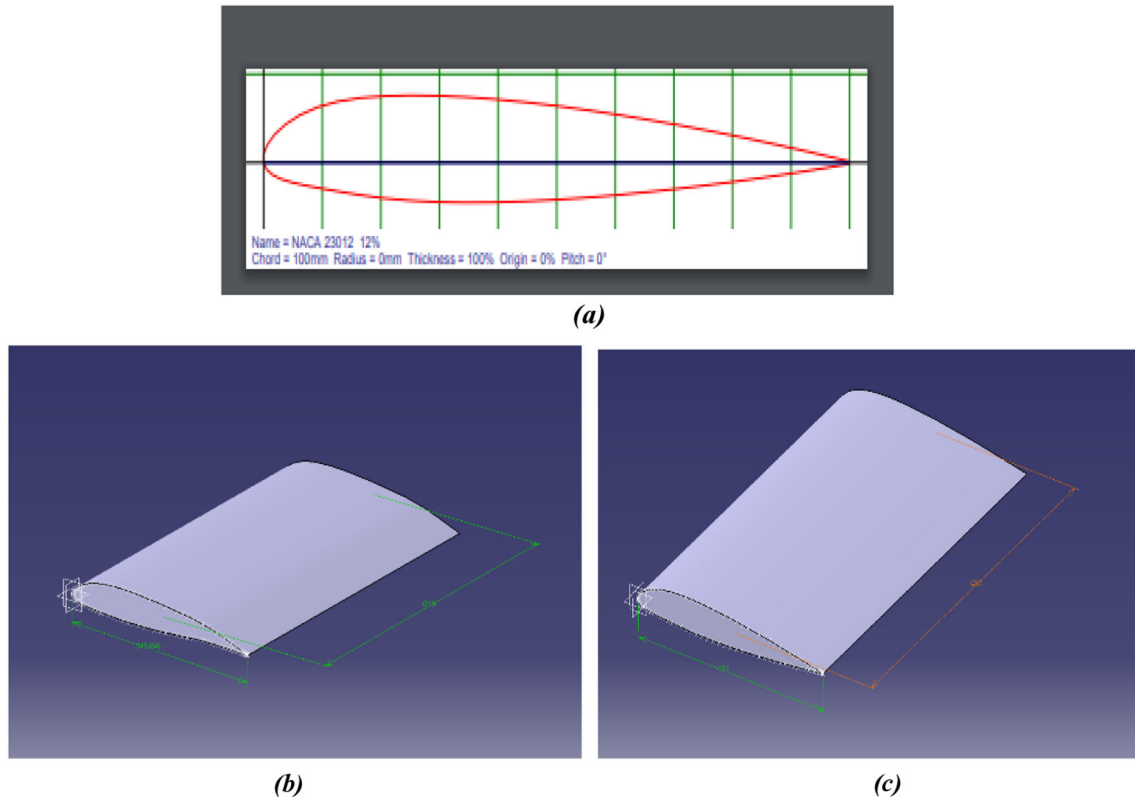


**Fig. 1** a Two-Dimensional airfoil. b, c CATIA model design of NACA2312 and baseline NACA 0012 Aerofoil (right)

and symmetrical aerofoil NACA 0012 are modeled in CATIA V5, as shown in Fig. 1. The morphing portion length is 25% from the trailing edge, and the total chord length is 150 mm. However, a study by Chen [24] confirmed that the chordwise variation in the cross-sectional area is essential.

Drela [25] developed Java Foil, an open-source flow simulation that analyses airfoil profiles and estimates airfoil characteristics quickly. The java foil has low initial complexity. As a result, the flow solvers prefer Java foil throughout the optimization method (Mauclère [26]; Morgado et al. [27]). For a particular (AoA), Reynolds number, and Mach number, Java foil calculates the lift and drag coefficients by Anitha et al. [28]. No value is recorded to the output file if there is no convergence when the software completes the solution method (Mauclère [26]). The coefficients lift and drag for the alpha sequence are computed in the Java FOIL program using the automated genetic process airfoil models.

## 2.5 Mathematical formulae

### 2.5.1 Basic formulations

In this study, a dimensionless analysis is working with Reynolds numbers.

$$Re = \frac{\rho v c}{\mu} \quad (1)$$

where  $\rho$ , density of the fluid;  $\theta$ , velocity of a fluid;  $c$ , length of the chord;  $\mu$ , dynamic viscosity and  $\nu$ , kinematic viscosity.

In most studies, coefficient of lift and drag are the two used parameters to evaluate the aerodynamic performance and are defined as:

$$Cl = \frac{2L}{\rho v^2 s} \quad (2)$$

$$Cd = \frac{2D}{\rho v^2 s} \quad (3)$$

where  $L$ , lift force;  $D$ , drag force and  $S$ , airfoil area.

The aerodynamic coefficient of forces is solved using conservation of equations., continuity, and momentum that are denoted as:

Mass conservation:

$$\nabla \cdot u = 0 \quad (4)$$

Momentum conservation

$$\frac{Du}{Dt} = -\nabla p + \mu \nabla^2 u + \rho \frac{Du}{Dt} F \quad (5)$$

where  $u$ , is the velocity vector, ( $\rho u = -\nabla + \mu \nabla^2 u$ ) represents the internal forces, and  $\rho F$  represents the external forces.

## 3 Computational setup and analysis

### 3.1 Grid generation

In this section, the mesh part describes and is based on previous studies in CFD, whereas the different grids for the morphed airfoil with its various deflections ( $\delta$ ). While selecting structural grids, various authors have selected structured grids to improve mesh size and quality, and they can be adapted to more complexity, as shown in Fig. 2. The Spalart–Allmaras CFD model simulates the aerodynamic performance of morphing wings based upon the pressure Reynold Averaged Naiver-Stokes equation. A second model upward scheme and a finite-difference technique have been used for convective and dissemination terms. The numerical domain's boundary has been set up as the far-field pressure barrier, and the surface has been designed as a no-slip-up stationary wall. Due to the trailing edge's significant intensity morphing, a local cell meshing approach and a spring-based smoothness process were used to upgrade the mesh. Following the method, the triangle types of cells were selected, and the control grid was processed around the airfoil to enhance the validity of the outcomes, as shown in Fig. 2.

We applied a mesh of local cell mesh generation approach together with user-provided parameters in our research to produce a continuous deviation of the trailing side. For example, in the descending deflection situation, the deflection angle changes from  $0^\circ$  to  $10^\circ$ , with  $f$  denoting its deflection frequencies (revolutions per second) and  $\theta$  indicating the trailing-maximum canon's deviation angle. During the deflection procedure, the portion of the airfoil chord from the remaining chord length is 25% unchanged. The grid node ( $x(t)$ ,  $y(t)$ ) of the morph airfoil may be determined with the help of the following equations.

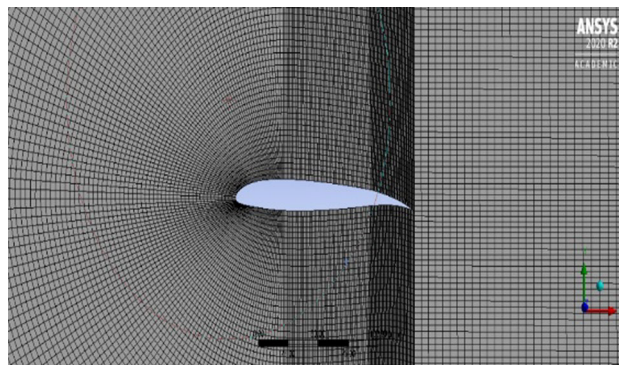


Fig. 2 Mesh generation of NACA 2312 2D airfoil model

$$\frac{\cos(\gamma^{n+1}(t))}{\cos(\gamma^n(t))} - 0.25 X(0.25) - x(t)^n = x^{n+1}(t) \quad (6)$$

Based on Eq. (6) the position of each node on the following trailing edges of the airfoil boundary varies during the morphing process, and the grid in the flowing fluid has reconstructed correspondingly. In the end, the trailing edge can extend continuously into the form of a curve. It is important to note that the Angle of Attack (AoA) remains constant during continuous trailing-edge deflection.

### 3.2 Model specifications, Mesh generation, and independent study

The study’s analytical findings are compared to the original and improved NACA 2312 airfoil profiles. The airfoil (c) has a chord length of 0.1 m. The Reynolds number (R) is set to  $10^4$ , and Spalart–Allmaras with a standard set of parameters is selected as a turbulence model. The SIMPLE method is used to manage the pressure–velocity interaction. All RANS equalities are discretized and used by a second-order upwind method. The simulations’ residual convergence level varies between  $10^{-3}$  and  $10^{-4}$ , depending on the airfoil angle of attack. Pressure far-field along the flow domain and wall along the airfoil has been assigned boundary conditions. Figure 2 illustrates the mesh parameters in the flow domain. The accuracy and analytical time are both influenced by mesh quality. It is broken into two components to create effective mesh grids in the numerical domain. The airfoil is dominated by a large mesh in the near-field area, with a radius of 5c. The term “far-field” corresponds to 12.5c from the computation domain’s origin. The overall mesh has two sizing possibilities: proximity and curvature. The edges are sized,

**Table 1** Mesh independence study for optimized airfoil at 0° AoA

Inlet velocity	V = 14.5 m/s	
	X component cos(α)	Y component sin(α)
Angle of attack	− 4° to 16°	
P <sub>0</sub> at the inlet and outlet	0	
Airfoil type	Wall	
Inlet	Velocity inlet	
Outlet	Pressure outlet	
Domain	C mesh	

and face sizing methods refine the mesh quality in the near-field area and around the airfoil. The flow is believed to be laminar, incompressible, stable, and two-dimensional. The gauge pressure is 0, and the outlet domain is set to pressure (Table 1).

## 4 Results and discussion

### 4.1 Most consistent aerodynamic physical properties of trailing-edge deflection

The flow domains and pressure distribution profiles of the morph and regular wings at 15° are determined to justify the differences in lift and drag coefficients. In Fig. 4a, b, the proportion on the top surface of the standard wing changes abruptly around a rebound view of the morphed trailing edge, whereas the coefficient pressures of both the morphed wings changes slowly. As a result, the coefficient of pressure (cp) contours of the morphed wing covers a higher area than those

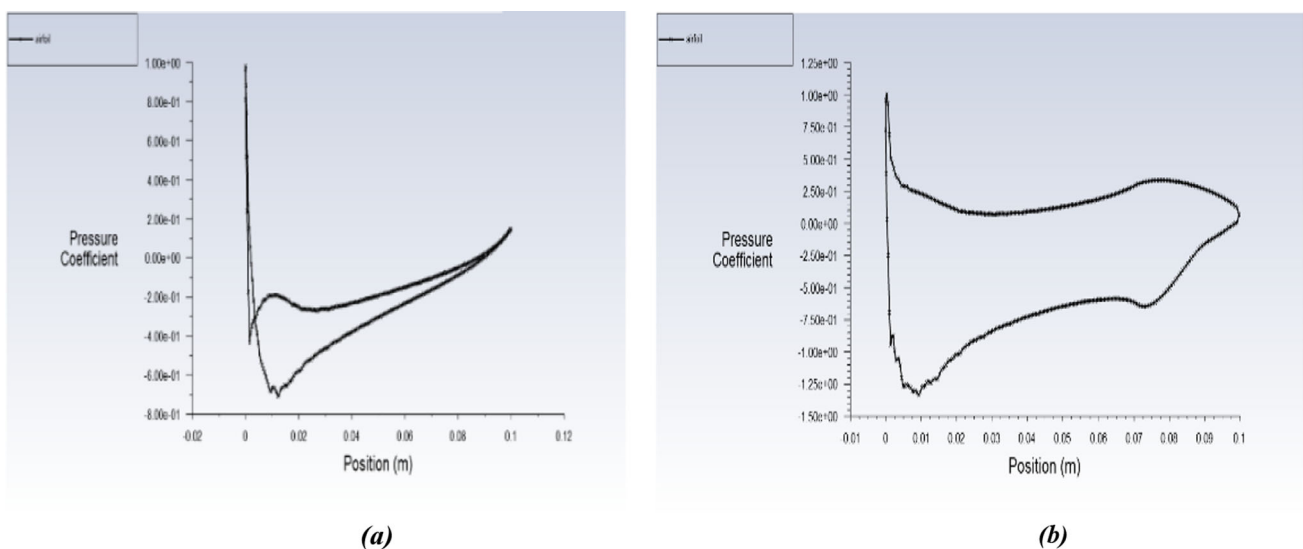


**Fig. 3 a, b** Comparison of Cp between morphing trailing edge and convention wing at  $\alpha = 15^\circ$

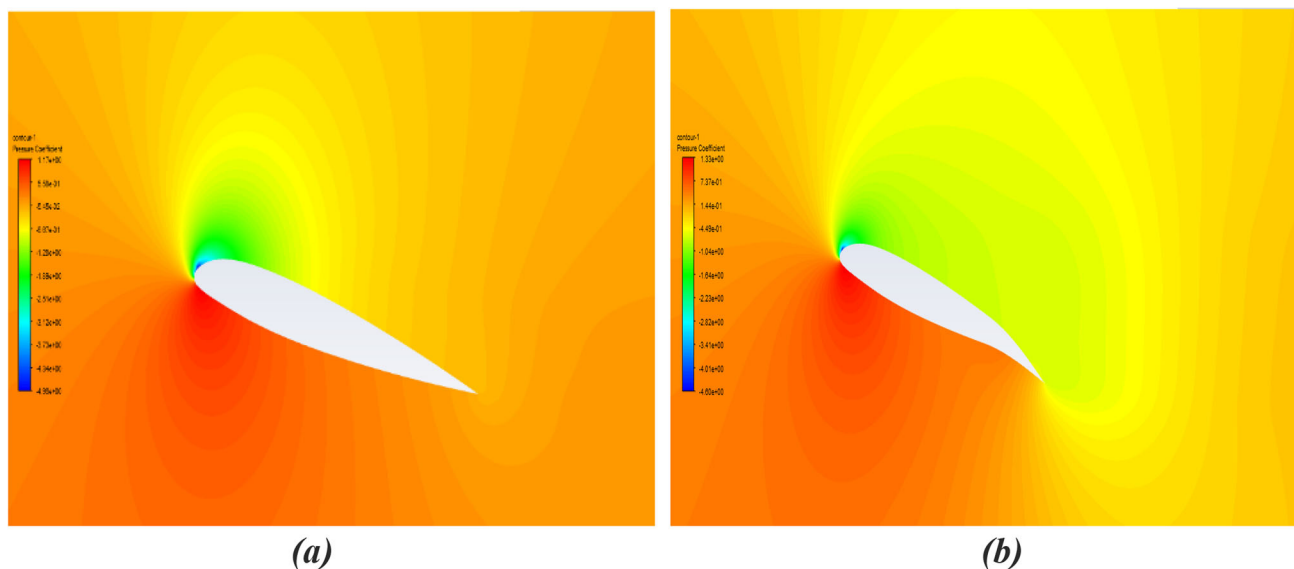


**Fig. 4** a, b Pressure fields conventional and morphing wings at  $\alpha = 15$

of a standard wing, resulting in a higher lift coefficient. In Fig. 3a, b, powerful vortices attach to the conventional wing's trailing edge from changing locations. However, the morphed wing has just a minimal vortex in the tail region. The flow separation is achieved early and much more forcibly in the conventional wing because of a sensible shift in the curve of the trailing edge side. In contrast, the constant altering of the rear edge can help to decrease the adverse difference in pressure, trying to attach the streamline to the wing surface. Research suggests that the morphed wing with a variable trailing edge outperforms the regular wing's aerodynamic efficiency (Fig. 4).

Comparison between morphed and traditional wings. The numerical properties of the varying MTE (morphing trailing edge) wing and the regular wing were investigated. The velocity flow is 14.5 m/s, respectively, while the morphing trailing edge deflection angle ranged from  $\delta = 2^\circ$  to  $10^\circ$ . Based on a micro aerial vehicle's condition, the velocity, considered about 14.5 m/s, is a deficient Reynolds number of 102,062.

#### 4.1.1 Pressure distribution

See Fig. 5.

#### 4.1.2 Velocity fields

See Fig. 6.

#### 4.1.3 Aerodynamic coefficient parameters

Figure 7a depicts the coefficient of lift curves of both standard and morphing wings. The changing or morphed wing's maximum lift slope is comparable to the regular wing. The morphed wing gives a more significant lift coefficient than the regular one, particularly near-crucial stalling angle. Consequently, the morphing wing's AoA and highest lift coefficient is higher than the conventional wing.

Furthermore, Fig. 7b depicts the coefficient of drag, which reveals that morphing wings with the lowest value are better for micro aerial vehicles than conventional wings. Although drag rises in subsequent wings, lift values are higher than drag when compared to conventional and morphing wings.

The L/D ratio of the two wings increased to its highest, as shown in Fig. 7c, then began to decline as the AoA (Alpha) increased. The morphed wing surpasses the traditional wing in provisions of the ratio L/D. The maximum L/D ratio of a morphing wing is 22.5 at an angle of attack is  $6^\circ$ , which would be 15.3% higher than a conventional wing's 19% at an AoA-angle of attack is  $8^\circ$ .

#### 4.2 The influence of MTE-deflecting angle on the aerodynamics of steady-state instances

At a deflection angle of  $16^\circ$ , Fig. 8a–c depicts the pressure on the deployment of the morphed airfoil with various trailing-edge deflection angles. The pressure allocations for the bottom surface of the wing are almost identical. However, the pressure on the top surface varied noticeably. With

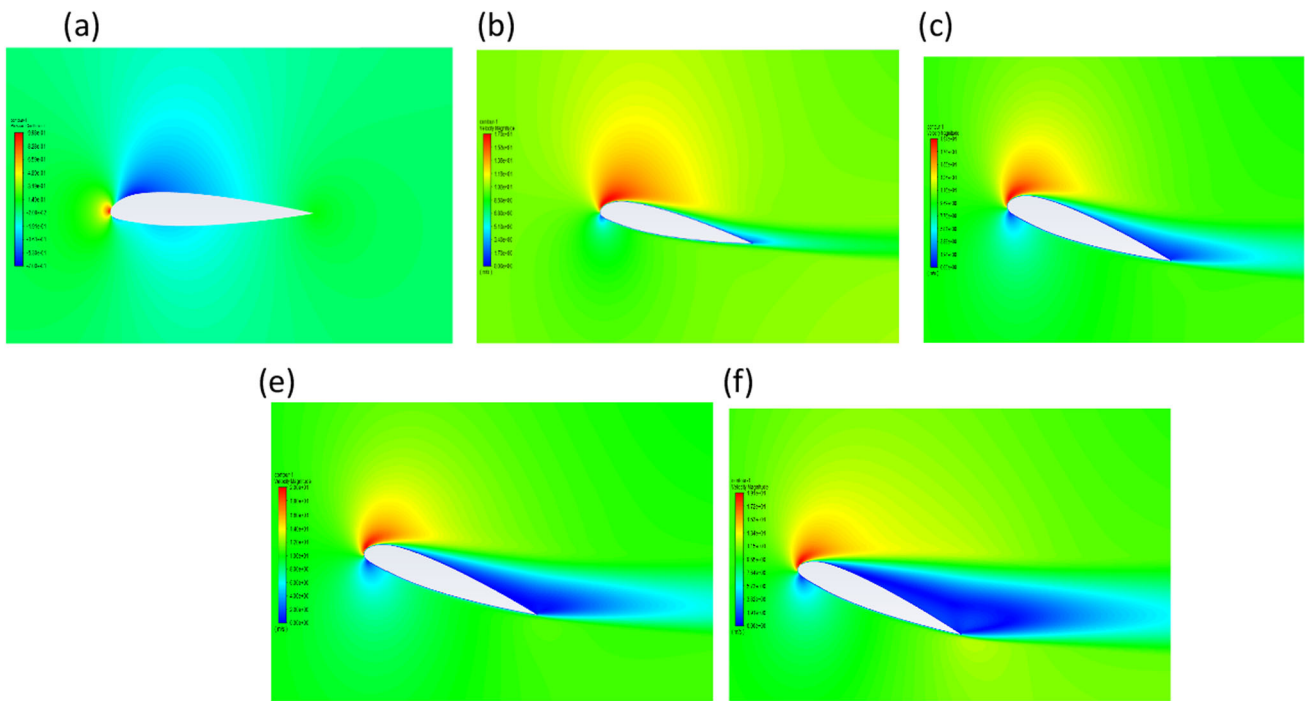


Fig. 5 Pressure fields for different angles of attack  $\alpha$  and without morphed deflection at velocity = 14.5 m/s

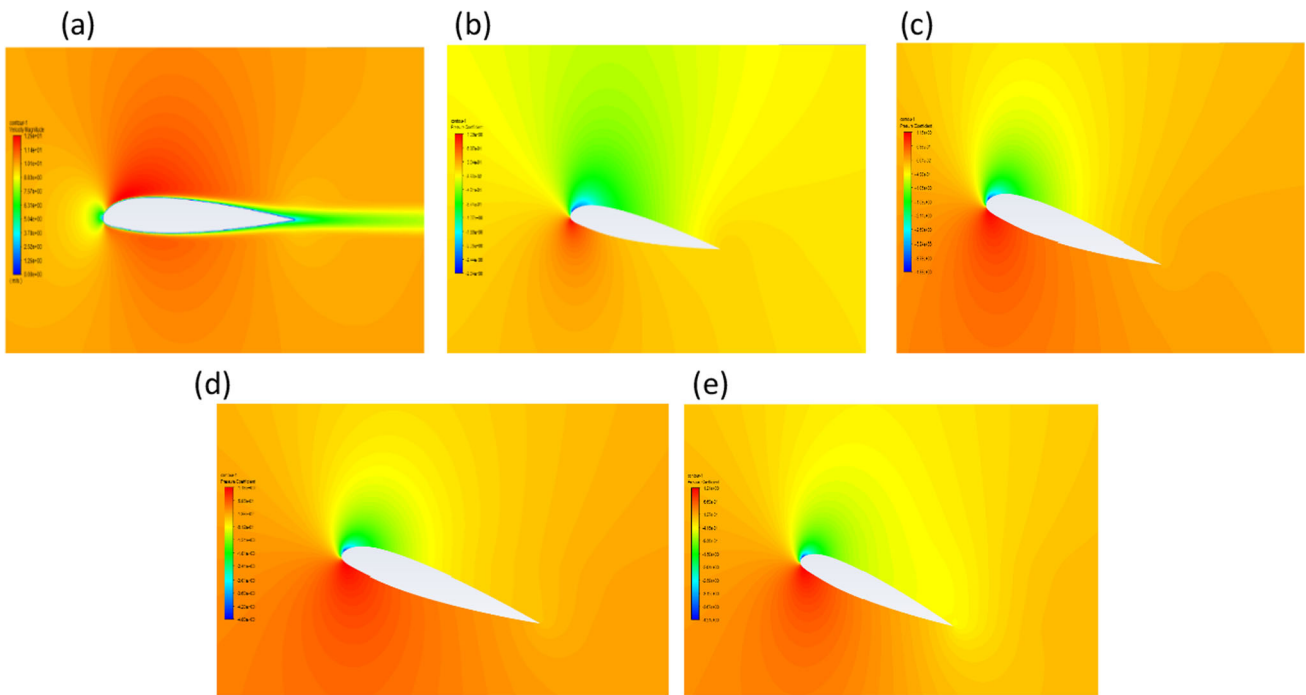
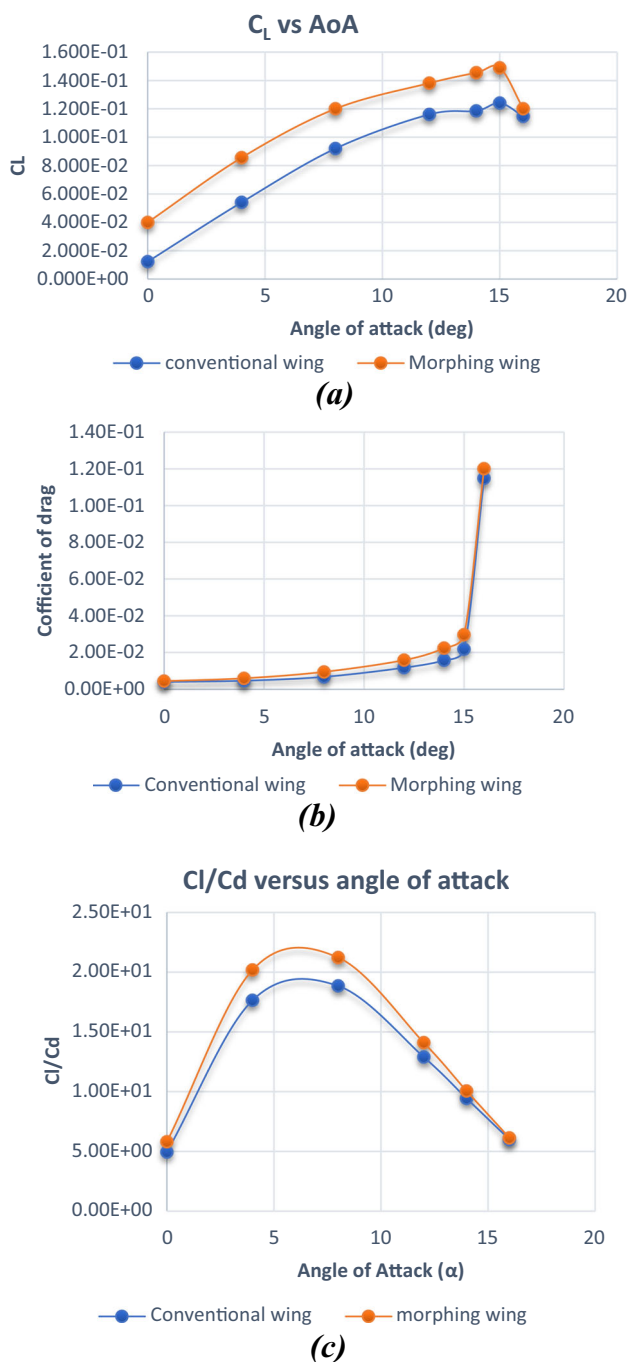


Fig. 6 Velocity fields for different angles of attack  $\alpha$  and without morphed deflection at velocity = 14.5 m/s



**Fig. 7 a–c** Comparison between conventional and morphing trailing edge wings. **a** Coefficient of Lift versus AoA-angle of attack for standard and morphing wing. **b** Coefficient of drag for standard and morphing wing. **c** Lift-to-drag ratio for conventional and morphing wing

the downward deflection, the region enclosed by the  $C_p$ -coefficient of pressure curves becomes more critical than a baseline for the airfoil ( $\delta = 0^\circ$ ).

Figure 9a, b depicts the aerodynamic forces at  $0^\circ$ ,  $5^\circ$ ,  $7^\circ$ , and  $10^\circ$  following trailing edge deflection angles. The stall angle is affected by the trailing-edge deflection, as illustrated in Fig. 9a, and the maximum coefficient of lift is reduced as a stalling angle of attack is reduced by the descending deflection of the trailing edge. The lift force coefficient and stalling angle of attack from the other side are boosted by the MTE-downward edge's deflection, as shown in Table 2. On the other hand, the downward deflection leads to an increasing nose-down coefficient of the moment ( $C_m$ ). The stronger the deflection- $\delta$  angle, the greater the lift and pitch-down coefficient pitch moment values. Additionally, the Fig. 9c shows the optimum lift-to-drag ratio changes the angle of attack attains  $6^\circ$ , and then when especially unlike standard aerofoil ( $\delta = 0^\circ$ ), the highest( $l/d$ ) proportion of the morphed wing together along by  $\beta = 7^\circ$  and  $\beta = 10^\circ$  increases by 1.8% and 12.5% correspondingly. The MTE descending deflection helps increase lift-to-drag ratio properties, but an upwards deviation also has the inverse result.

## 5 Conclusions

The static aerodynamics parameters with morphed and conventional wings were investigated in this study, and the static aerodynamic features of a morphed wing in a variable trailing edge. These two characteristics' effects on the lift's stable coefficient were discussed with an MTE-morphing trailing edge deflection angle.

- Before stall occurs, when such movable trailing edge bounces lower, the morphed wing has a more significant lift and drag coefficient and a higher lift-to-drag ratio than a traditional wing.
- The steady streamlined flow parameters and the versatile trailing edge's deformation have a negligible impact on aerodynamics at a small AoA. The trailing edge deflections affect at stall angle feature. Descending deflection of the trailing edge enhances the stalling AoA. Furthermore, increasing the downstream deflection angle improves the morphing wing's lift-to-drag ratio as the angle of attack decreases.
- At a smaller AoA, the variable trailing edge's deviation has a negligible effect on stable aerodynamic performance. The trailing-edge deflection primarily influences the stall characteristics. The stall occurs when the descending deflection of the morphed trailing edge increments the AoA-angle of attack. Furthermore, the higher the



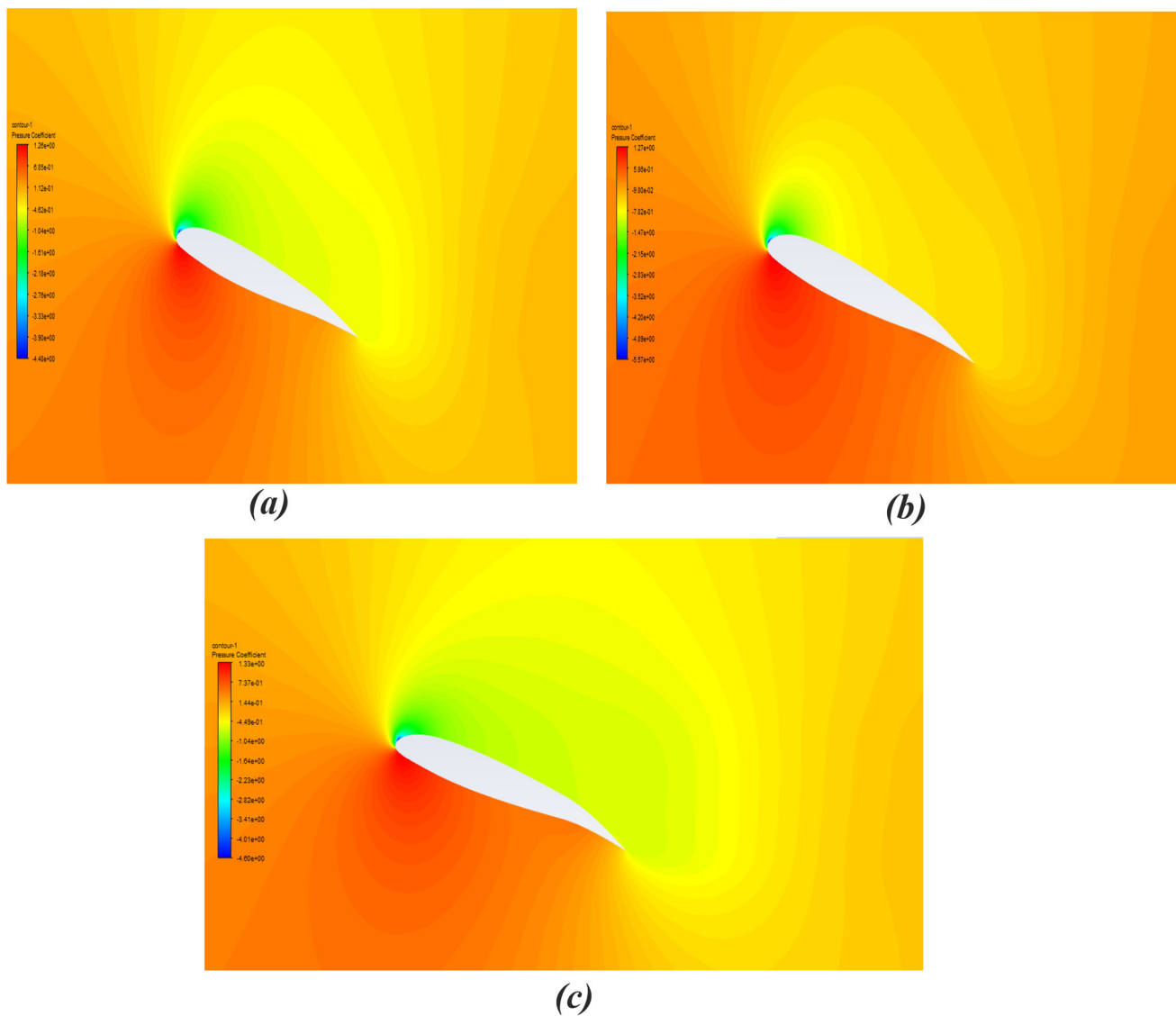


**Fig. 8** Flow field and Pressure contours with morphing trailing-edge deflections angle at  $\alpha = 15$  deg. **a** MTE- deflection at  $\delta = 5$  deg, **b** MTE-deflection at  $\delta = 7$  deg, **c** MTE deflection at  $\delta = 10$  degrees

downward deflection angle, the better its morphing wing's lift-to-drag (L/D) ratio is at a low attack angle.

- The coefficients obtained from the flow simulation and optimization studies are the same. The Cl/Cd ratio has been enhanced for AoA in the studies, although the study is one objective to optimize. In conclusion, despite the study being a single objective optimization study, many results were obtained to boost the lift coefficient.
- In the future, we'll start experimenting with actuation mechanics to morph the trailing edge to employ more suitable or flexible materials to control the morphing wing two-dimensionally for additional confirmation with sim-

ulated outcomes. The parameters determined via flow optimization studies are the same.

- Despite the data from single optimization research, the Cl/Cd ratios have improved for numerous AoA investigations. Even though the study was a single objective optimization study, several results were produced on enhancing the lift coefficient.
- Finally, the same airfoil might be subjected to multi-objective optimization research, and the results observed in future work. The lift and drag coefficients may be determined experimentally using the optimized airfoil profile.

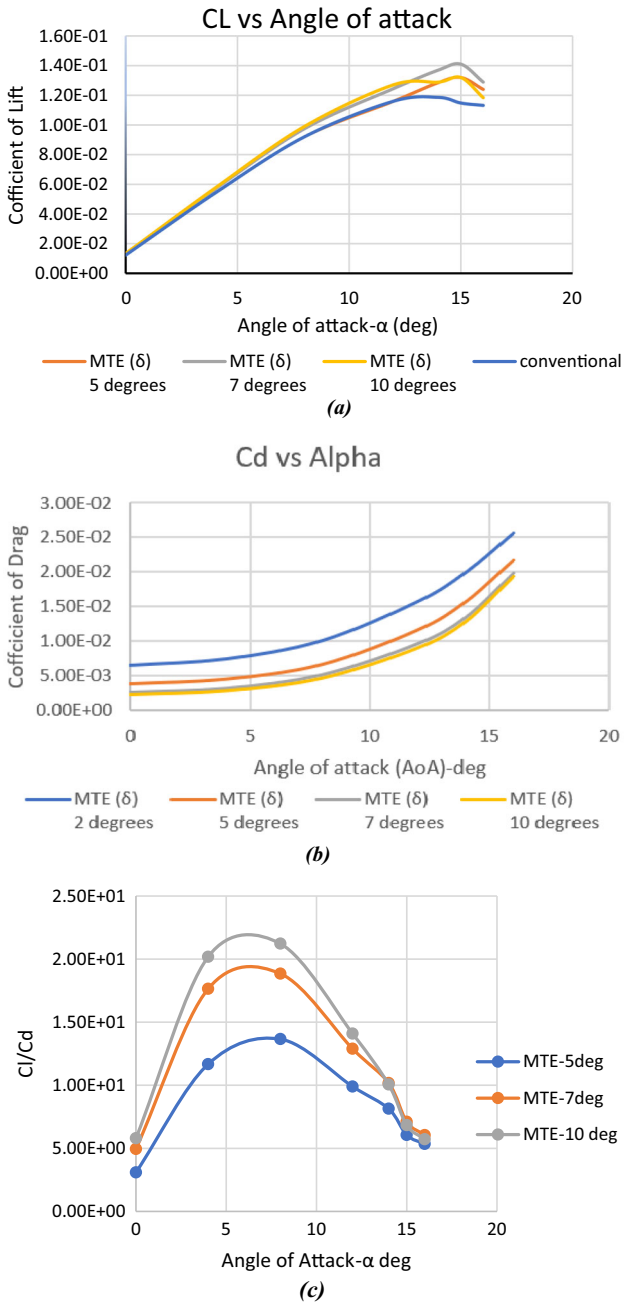


**Fig. 9 a** Coefficient of lift and AoA varying with different Morphing trailing edges (MTE) deflections angles at velocity = 14.5 m/s. **b** Coefficient of drag versus AoA-angle of attack. **c** Lift-to-Drag ratio vs AoA-(Angle of attack) varies at different MTE deflections

**Table 2** Shows the values of  $C_l$  versus AoA varying for different morphing trailing edge and an angle of attack at velocity = 14.5 m/s

AoA-Angle of attack	Conventional flap	MTE-Morphed trailing edge-(δ) 5°	MTE-Morphed trailing edge-(δ) 7°	MTE-Morphed trailing edge-(δ) 10°
0	$1.227 \cdot 10^{-2}$	$1.23 \cdot 10^{-2}$	$1.31 \cdot 10^{-2}$	$1.33 \cdot 10^{-2}$
4	$5.408 \cdot 10^{-2}$	$5.41 \cdot 10^{-2}$	$5.68 \cdot 10^{-2}$	$5.75 \cdot 10^{-2}$
8	$9.202 \cdot 10^{-2}$	$9.20 \cdot 10^{-1}$	$9.75 \cdot 10^{-2}$	$9.90 \cdot 10^{-2}$
12	$1.161 \cdot 10^{-1}$	$1.1 \cdot 10^{-1}$	$1.25 \cdot 10^{-1}$	$1.27 \cdot 10^{-1}$
14	$1.186 \cdot 10^{-1}$	$1.29 \cdot 10^{-1}$	$1.37 \cdot 10^{-1}$	$1.29 \cdot 10^{-1}$
15	$1.148 \cdot 10^{-1}$	$1.32 \cdot 10^{-1}$	$1.41 \cdot 10^{-1}$	$1.32 \cdot 10^{-1}$
16	$1.132 \cdot 10^{-1}$	$1.24 \cdot 10^{-1}$	$1.29 \cdot 10^{-1}$	$1.18 \cdot 10^{-1}$

## References

- Li, D., Zhao, S., Ranch, A.D., et al.: A review of modeling and analysis of morphing wings. *Prog. Aerosp. Sci.* **100**, 46–62 (2018)
- Koreanschi, A., Gabor, O.S., Acotto, J., et al.: Optimization and design of an aircraft's morphing wing-tip demonstrator for drag reduction at low speeds, Part II—experimental validation using Infra-Red transition measurement from Wind Tunnel tests. *Chin. J. Aeronaut.* **30**(1), 164–174 (2017)
- Gabor, O.S., Koreanschi, A., Botez, R.M., et al.: Numerical simulation, and wind tunnel tests investigation and validation of a morphing wing-tip demonstrator aerodynamic performance. *Aerosp. Sci. Technol.* **53**, 136–153 (2016)
- Abdessemed, C., Yao, Y., Bouferrouk, A., et al.: Morphing airfoils analysis using dynamic meshing. *Int. J. Math. Heat Fluid Flow* **28**(5), 1117–1133 (2018)
- Ai, Q., Jawahar, H.K., Azarpeyvand, M. Experimental investigation of the aerodynamic performance of airfoils fitted with morphing trailing edges. In: 54th AIAA Aerospace Sciences Meeting; San Diego, USA, pp. 1–13. AIAA, Reston. 4–8 Jan 2016
- Jawahar, K.H., Ai, Q., Azarpeyvand, M.: Experimental and numerical investigation of aerodynamic performance for airfoils with morphed trailing edges. *Renew. Energy* **127**, 355–367 (2018)
- Lim, H.W., Kim, H.: Multi-objective airfoil shape optimization using an adaptive hybrid evolutionary algorithm. *Aerosp. Sci. Technol.* **87**, 141–153 (2019). <https://doi.org/10.1016/j.ast.2019.02.016>
- Jeong, J.H., Kim, S.H.: Optimization of thick wind turbine airfoils using a genetic algorithm. *J. Mech. Sci. Technol.* **32**(7), 3191–3199 (2018). <https://doi.org/10.1007/s12206-018-0622-x>
- Tandis, E., Assareh, E.: Inverse design of airfoils via an intelligent hybrid optimization technique. *Eng. Comput.* **33**(3), 361–374 (2017). <https://doi.org/10.1007/s00366-016-0478-6>
- Yang, F., Yue, Z., Li, L., Yang, W.: An aerodynamic optimization method based on the Bezier curve and radial basis function. *Proc. Inst. Mech. Eng. Part G J. Aerosp. Eng.* **232**(3), 459–471 (2018)
- Fincham, J.H.S., Friswell, M.I.: Aerodynamic optimization of a camber morphing aerofoil. *Aerosp. Sci. Technol.* **43**, 245–255 (2015)
- Della Vecchia, P., Daniele, E., D'Amato, E.: PARSEC parameterization and an evolutionary algorithm are used to optimize the form of an airfoil. *Aerosp. Sci. Technol.* **32**(1), 103–110 (2019)
- Mukesh, R., Lingadurai, K., Selvakumar, U.: Airfoil shape optimization using non-traditional optimization techniques and its validation. *J. King Saud Univ. Eng. Sci.* **26**(2), 191–197 (2014)
- Salunke, N.P., Junaid Ahamad, R.A., Channiwala, S.A.: Airfoil parameterization techniques: a review. *Am. J. Mech. Eng.* **2**(4), 99–102 (2014)
- Ebrahimi, M., Jahangirian, A.: Aerodynamic optimization of airfoils using adaptive parameterization and genetic algorithm. *J. Optim. Theory Appl.* **162**(1), 257–271 (2014)
- Melin, T.: Parametric Airfoil Catalog, Part II: Göttingen 673 to YS930: An Aerodynamic and Geometric Comparison Between Parametrized and Point Cloud Airfoils. Linköping University Electronic Press, Linköping (2013)
- Niu, W., Zhang, Y., Chen, H., Zhang, M.: Numerical study of a supercritical aerofoil/wing with variable-camber technology. *Chin. J. Aeronaut.* **33**(7), 1850–1866 (2020)
- Dumont, A.: Adjoint-based aerodynamic shape optimization applied to morphing technology on a regional aircraft wing. In: Concilio, A., Dimino, I., Lecce, L., Pecora, R. (eds.) *Morphing Wing Technologies Large Commercial Aircraft and Civil Helicopters*, pp. 145–174. Butterworth-Heinemann, Oxford (2018)
- Zhou, H., Zhu, H., Main, H.H., Wang, G. Modelling and aerodynamic prediction of fish bone active camber morphing aerofoil. In: *Proceedings of 2018 15th International Bhurban Conference on Applied Sciences and Technology, Islamabad, Pakistan*. <https://doi.org/10.1109/IBCAST.2018.8312280>. 9–13 Jan 2018
- Woods, B.K.S., Fincham, J.H.S., Friswell, M.I. Aerodynamic modeling of the active fishbone camber morphing concept. In: *Proceedings of the RAeS Applied Aerodynamics Conference, Bristol, UK*. 22–24 July 2014
- Huntley, S.J., Woods, B.K., Allen, C.B. Computational analysis of the aerodynamics of camber morphing. In: *AIAA Aviation 2019 Forum, Dallas, Texas*. 17–21 June 2019
- Sun, J., Guan, Q., Liu, Y., et al.: Morphing aircraft based on smart materials and structures: a state-of-the-art review. *J. Intell. Mater. Syst. Struct.* **27**(17), 2289–2312 (2016)
- Kaul, U.K., Nguyen, N.T.: Drag optimization study of variable camber continuous trailing edge flap (VCCTEF) using OVERFLOW. In: *32nd AIAA Applied Aerodynamics Conference, Atlanta, GA*. 16–20 June 2014
- Wang, C., Haddad Khodaparast, H., Friswell, M.I., Shaw, A.D., Xia, Y., Walters, P.: Development of a morphing wingtip based on compliant structures. *J. Intell. Mater. Syst. Struct.* **29**(16), 3293–3304 (2018)
- Drela, M.: XFOIL: An analysis and design system for low Reynolds number airfoils. In: Mueller, T.J. (eds) *Low Reynolds Number Aerodynamics. Lecture Notes in Engineering*, vol 54. Springer, Berlin, Heidelberg (1989)
- Mauclère, X.: Automatic 2D airfoil generation, evaluation and optimisation using MATLAB and XFOIL (2009)
- Morgado, J., Vizinho, R., Silvestre, M.A.R., Pscoa, J.C.: CFD performance predictions for high lift low Reynolds number airfoils. *Aerosp. Sci. Technol.* **52**, 207–214 (2016)
- Anitha, D., Shamili, G.K., Ravi Kumar, P., Sabari Vihar, R.: Airfoil shape optimization using Cfd and parametrization methods. *Mater. Today Proc. Part I* **5**(2), 5364–5373 (2018)

**Publisher's Note** Springer Nature remains neutral with regard to jurisdictional claims in published maps and institutional affiliations.

Springer Nature or its licensor (e.g. a society or other partner) holds exclusive rights to this article under a publishing agreement with the author(s) or other rightsholder(s); author self-archiving of the accepted manuscript version of this article is solely governed by the terms of such publishing agreement and applicable law.